Space/Time Quantitation of Thallium-201 Myocardial Scintigraphy

Ernest Garcia, Jamshid Maddahi, Daniel Berman, and Alan Waxman

Cedars Sinai Medical Center and University of California, Los Angeles, California

A comprehensive method is described for quantitation of the spatial distribution of Tl-201 in the myocardium and its changes with time. The method, applied here to 51 patients, uses bilinear interpolative background subtraction to compensate for tissue crosstalk, and circumferential profiles to quantitate the relative radionuclide activity in the myocardium as an angular function with origin at the center of the left-ventricular cavity. In addition, washout circumferential profiles are calculated as percent washout from the stress circumferential profiles. Abnormal thallium distribution or washout is identified by automatic computer comparison of each patient's profiles with the corresponding limits of normal profiles, determined from the pooled profiles of 31 normal patients. In these 31, the computer output was normal in all cases. In 20 patients with angiographically documented coronary artery disease, 19 were determined to be abnormal by this method. This new computerized treatment provides accurate objective assessment of the presence of coronary artery disease.

J Nucl Med 22: 309–317, 1981

Sequential thallium-201 scintigraphy following injection at peak exercise has achieved widespread use for the detection of coronary artery disease (*1*). Despite increasing availability of nuclear medicine computer systems, current evaluation of regional myocardial perfusion is usually made by visual interpretation of analog Tl-201 images. This approach is limited by observer variability, dependence on the quality of the hard-copy output, and the inability to compensate for tissue crosstalk. Recently, several approaches have provided significant contributions to the development of a quantitative method of Tl-201 interpretation (*2-5*), but each approach has limitations. Therefore, we have developed a comprehensive computerized method to express objectively, as a function of space and time, the relative distribution of Tl-201 in the myocardium. The purpose of this report is to describe the method and to evaluate the results in normal patients and in patients with coronary artery disease (CAD).

Received June 9, 1980; revision accepted Nov. 17, 1980.

For reprints contact: Daniel S. Berman, MD, Director, Nuclear Cardiology, Cedars-Sinai Medical Center, 8700 Beverly Blvd., Los Angeles, CA 90048.

METHODS

Patient selection. Two groups of patients were studied. Group A consisted of 31 patients referred to this institution for assessment of possible CAD. This group included 21 males and ten females ranging in age from 26 to 73 yr (mean age 49 yr). These patients were classified as normal by having less than 1% likelihood of coronary artery disease as judged by sequential Bayesian analysis (*6*) of age, sex, symptom classification, and the results of multiple noninvasive stress tests other than Tl-201 scintigraphy. In our laboratory these tests were the exercise electrocardiogram, cardiokymogram (*7*), and fluoroscopic assessment of coronary calcification. Group B consisted of 20 consecutive patients who underwent both Tl-201 scintigraphy and coronary arteriography, and whose arteriographic studies revealed greater than 50% luminal stenosis of at least one of the three major coronary arteries. This group included 18 males and two females ranging in age from 36 to 76 yr with a mean age of 58 yr. Ten patients had triple-vessel disease, six double, and four single-vessel disease. Of the Group B patients, 11 had prior myocardial infarction.

Exercise and imaging procedure. Patients in Groups

A and B underwent stress and redistribution thallium-201 myocardial scintigraphy as part of a routine diagnostic evaluation. They were stressed using a multistage treadmill test, according to the Bruce protocol. Exercise was maximal, terminated only after the patient developed chest pain, exhaustion, serious arrhythmia, or hypotension. A dose of 2 mCi of thallium-201 was injected at maximum exercise, and the patients continued to exercise for 45–90 sec after injection. Following exercise, multiple-view myocardial scintigrams were obtained serially, at approximately 6 and 40 min, 3–6 hr, and frequently 18–24 hr, after the injection of thallium. During each phase of imaging, 10-min images were obtained in the anterior, 45° and 70° left anterior oblique (LAO) projections. Imaging was performed using a standard-field Anger camera equipped with 37 photomultiplier tubes, a 0.25 in. thick NaI(Tl) crystal, and a high-resolution, parallel-hole collimator. A 25% energy window centered on the 80-keV x-ray peak was used, with an independent 15% window centered on the 167-keV photopeak. All images were stored on magnetic disk in a 128 × 128, 8-bit matrix.

Computer processing and analysis. Each image is compensated for tissue crosstalk by performing bilinear interpolative background subtraction as described by Goris et al. (*8*). For this purpose, a rectangular boundary enclosing the heart was positioned by the computer operator approximately 4 pixels away from the myocardium (Fig. 1). The background subtraction method was modified by use of a proximity weighting function described by Watson et al. (*9*). The effect of this modification is to produce a more rapid fall-off of the computed tissue crosstalk, this being particularly important where the rectangle surrounding the myocardium, assigned as the origin of background, crosses areas of higher uptake, such as the liver (*9*).

After background subtraction, the images are smoothed using a standard algorithm for nine-point weighted averaging. From these images, circumferential

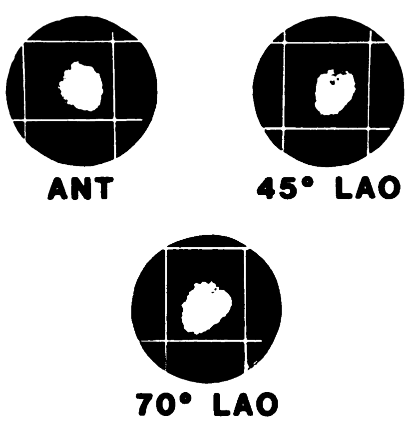

FIG. 1. Placement of rectangular boundary relative to the heart used for performing bilinear interpolative background subtraction in the anterior (ANT), and 45° and 70° LAO projections.

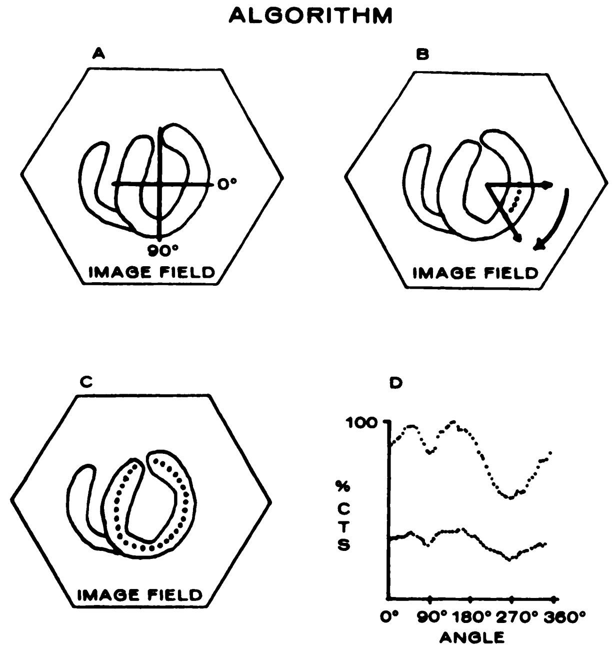

FIG. 2. Diagrammatic representation of method for obtaining circumferential profiles of the myocardium. Polar coordinate reference axis is shown in (A). Image pixels for circumferential profile analysis are found by performing a radial search for maximum value at 6° intervals (B) throughout 360°. Maximal values shown as black dots in (B) and (C) are then replotted in (D) for each angle as a percentage of the maximum value for the circumferential profile. Top curve in (D) represents circumferential profile from stress thallium-201 image; below, that from the 4-hr delayed image.

maximal-count profiles of the myocardial distribution of Tl-201 are obtained (Fig. 2) in a manner similar to that proposed by Vogel et al. (*3*) and Meade et al. (*2*). Each point in these profiles represents the maximum counts per pixel along a radius traversing the myocardium. The profile is constructed by the computer from the values of 60 radii spaced at 6° intervals plotted clockwise. These profiles quantitate the segmental activity as an angular function referenced from the visually located center of the left ventricular cavity. The operator also assigns the maximum radius to which the computer will search. This is done to prevent the algorithm from searching outside the left-ventricular myocardium into other structures such as the right ventricle. These circumferential profiles (CP) are then aligned (*4*). The computer operator identifies the location of the scintigraphic apex on the circumferential profile by visual inspection of the stress images as well as inspection of the shape of the stress profile relative to that of the redistribution profile. The computer then automatically shifts that point in the circumferential profile to coincide with 90°. These profiles are subsequently plotted for each view at each time interval. The curves were normalized to the maximum pixel value found in any of the profiles.

In addition to the distribution profiles, washout circumferential profiles (WCP) are calculated as percent washout from stress for the 40-min, and 4- and 24-hr intervals.

$$\mathrm{WCP}\,(\theta,t) = \frac{\mathrm{CP}\,(\theta,s) - \mathrm{CP}\,(\theta,t)}{\mathrm{CP}\,(\theta,s)} \times 100 \qquad (1)$$

where the WCP (θ,t) is the washout from a myocardial segment, θ, at time t and s represents the time of immediate post-stress imaging. The time required for computer processing averaged 15 min per patient.

Definition of normal limits. The mean value and standard deviation were established from the pooled data of the 31 normal patients for each of the 60 angular locations of the anterior, 45° LAO, and 70° LAO images for each time interval. The actual time at which the stress views and redistribution views were obtained was used to interpolate the redistribution circumferential profiles and washout circumferential profiles to exactly 4 hr. This was done for each normal patient by assuming a monoexponential normal washout (*10*) between stress and redistribution during the actual imaging delay, and correcting to 4 hr using the following decay formula:

$$\mathrm{CP}\,(\theta,4) = \mathrm{CP}\,(\theta,\Delta t)\, e^{\frac{0.693}{\bar{t}_{1/2}}(\Delta t - 4)} \qquad (2)$$

where $\Delta t = t - s$, delay (in hours) between beginning of stress imaging and redistribution and $\bar{t}_{1/2}$ = patient's mean effective half-time. $\bar{t}_{1/2}$ was calculated as follows:

$$\bar{t}_{1/2} = \frac{\sum_{\theta=1}^{60} t_{1/2}\,(\theta)}{60} \qquad (3)$$

where

$$\bar{t}_{1/2}\,(\theta) = \frac{0.693\,\Delta t}{\ln\left[\frac{\mathrm{CP}\,(\theta,s)}{\mathrm{CP}\,(\theta,t)}\right]}. \qquad (4)$$

For the distribution profiles, normal limits were defined as the curves representing two standard deviations below the mean, and were used as the threshold for defect detection. These curves were obtained by averaging the profiles of each view, point by point, around the circumference of the left ventricle and calculating the standard deviation for each point. Similarly for the washout profiles both 1- and 4-hr normal washout limits were defined from curves representing 2 s.d. below the mean for those intervals. In addition, the mean effective half-time was calculated in each view for each of the 60 angular locations. These criteria using 2 s.d. with a one-tailed analysis statistically encompass 97.5% of the population.

Quantitative interpretation. Initial distribution and washout circumferential profiles for the 31 normals and the 20 patients with CAD were interpreted by a computer program that compared each curve, aligned at the apex, with the empirically determined normal limits described above. This diagnostic program printed out the angular locations of each profile that were outside normal limits.

Various quantitative criteria for abnormality were applied to patients in Group A and Group B, and the criteria that best separated the normals from the patients with CAD were defined. These criteria were applied to any part of the patient's profile in which two or more consecutive 6° arcs fell outside normal limits (2 s.d. beyond the mean curve). The following criteria for abnormality of the circumferential profiles were evaluated:

1. Stress profile below the normal limits, indicating an initial defect;
2. Early redistribution profile more than 2 s.d. above the mean of normals and/or early washout profile (40 min after injection) below the normal early washout limit. These criteria correspond to "late peaking" myocardial uptake of Tl-201; and
3. 4-hr redistribution profile above the normal limits and/or 4-hr washout profile more than 2 s.d. below the mean normal washout profile. These criteria correspond to "slow washout" of Tl-201 in 4 hr.

The normal limits of the distribution and washout corresponding to the 4-hr delayed images were corrected to the actual imaging time (2.5–6.5 hr) by solving for CP(θ,t) from Eq. 2.

RESULTS

The normal distribution and washout characteristics, and the associated standard deviations above and below the normal mean curve, are illustrated in Figs. 3A and B, respectively. The circumferential profiles for each view and for each time show similar characteristic shapes. There is noticeably reduced radioactivity at the apex and at the base of the left-ventricular myocardium. The minimum lower limit of normal value for the thallium distribution at stress along the segments considered for interpretation (330–210°) was 56% of the maximum and corresponded to the apex in the 45° LAO view. The standard deviations calculated for each mean profile showed regional variations. In general there was a larger error along the basal region and smaller error along the apical regions. This is partly because the apex was used for alignment, and thus one would expect more reproducible results closer to that location.

When comparing the circumferential profile at stress with the profile obtained at a later time, we find an apparent damping effect due to the nature of the normalization process. Actually, if the profile from a later time is normalized so that its maximum point is equal to the maximum point of the stress profiles, both profiles coincide exactly. This indicates that the relative Tl-201 distribution observed in the stress profiles is maintained in normal patients at the later imaging times, and thus that every portion of the myocardium washes out at the

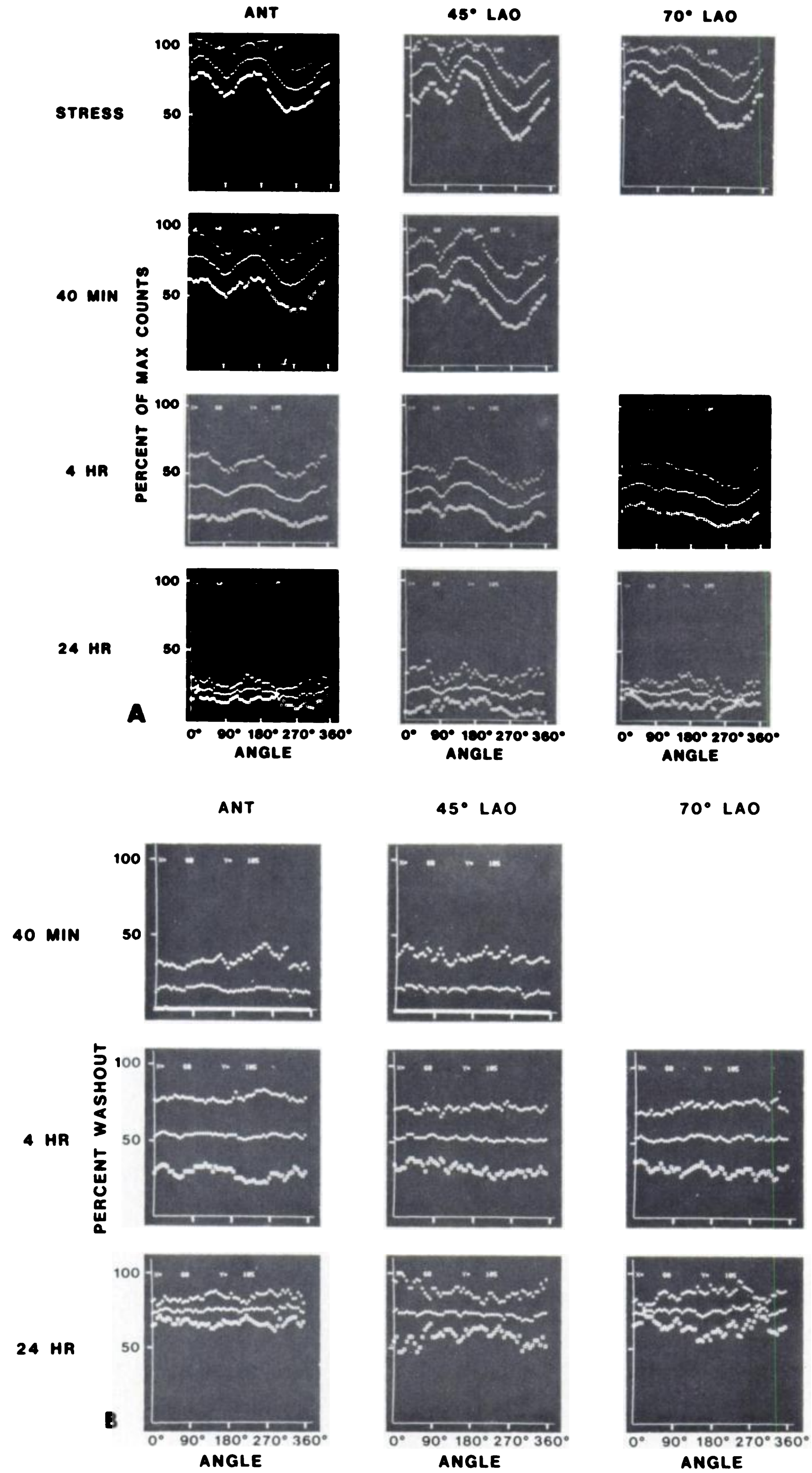

FIG. 3. (A) Distribution circumferential profiles representing mean ± 2 s.d. from each view, at each time interval, in a group of 31 normal patients. Mean curves, lying between other two are plotted with "+." Forty-minute images in 70° LAO are not performed. (B) Washout circumferential profiles representing mean ± 2 s.d. from each view, at each time interval, in same group of normal patients used in part A.

same rate. This finding is the reason for the horizontal line appearance of the washout circumferential profiles shown in Fig. 3B. The mean effective half-time (which because of the long $t_{1/2}$ of Tl-201 is largely due to washout) was calculated for each of the 60 angular locations using Eq. 4. The mean effective half-time, with 2 s.d. above and below the mean, is shown in Fig. 4. The mean effective half-time was found to be very similar for each view and for each location in the myocardium, namely 3.97 ± 1.3 hr.

The following criteria best separated normals from the patients with CAD:

1. An "initial defect" was defined by any 18° segment (three contiguous radii) of the stress profile falling below the normal limit;
2. "slow washout" was defined by any 18° segment (three contiguous radii) of the 4-hr washout profile falling below the normal limit; and
3. to be considered abnormal, the patient needed at least two abnormal 18° arcs in the combined initial distribution and washout profiles in the three views. Neither of the criteria corresponding to "late peaking" of regional uptake alone further discriminated CAD patients from normals.

Using the above criteria, quantitative analysis of Tl-201 images was normal in all 31 normal patients and was abnormal in 19 of 20 CAD patients. A characteristic, normal example is shown in Figs. 5 and 6. Two of the 19 CAD patients were detected by the 4-hr washout criterion alone. Importantly, 19 of 61 abnormal myocardial segments were detected by this washout criterion without initial defects. Figures 7 and 8 illustrate a patient with triple-vessel CAD in whom the extent of abnormality is detected only by the quantitative washout criterion; there was no quantitative initial defect or visible abnormality in the unprocessed images. The 45° LAO processed images (Figs. 7B and 8B) demonstrated a possible reversible defect in the posterolateral wall, suggesting the presence of disease, but underestimating disease extent.

Sequential thallium-201 scintigrams from eleven patients, five with and six without CAD, were analyzed by two independent computer operators. Each of the three views was divided into three segments for a total of nine segments per patient. Each segment was analyzed by the computer as to whether it was normal or abnormal using the initial-defect and/or slow-washout criteria described above. Concordant results were obtained by the two operators in 93 of the 99 segments. In the six patients without CAD, agreement was found in all 54 normal segments. In the five patients with CAD, the results were as follows: there was agreement in 19 segments as being normal, 20 segments as being abnormal, and six disagreements. Table 1 illustrates the results by segment of this reproducibility study. The main cause of discrepancy was slight variation in aligning the apex at 90° in the patients with large apical defects.

DISCUSSION

It is well recognized that one of the more pressing needs in the area of thallium myocardial imaging is the standardization of the interpretation of scintigrams. Objective criteria for the detection and assessment of extent of CAD can come only from a quantitative technique. The present investigation utilizes a combination of the attributes of several methods previously described in the literature (*2–5*), and incorporates the use of serial Bayesian analysis to identify normal patients as well as the use of washout circumferential profiles to analyze myocardial washout characteristics.

This method of space/time quantitation of myocardial Tl-201 uses a computer to (a) process the scintigrams; (b) measure and display maximal circumferential profiles corresponding to the Tl-201 distribution in the myocardium at different times; (c) measure and display the washout circumferential profiles; and (d) compare each patient's profiles with previously established normal limits and print out the extent (in degrees) and intensity (in percentage) of those segments below these normal limits.

The image processing performed consisted primarily

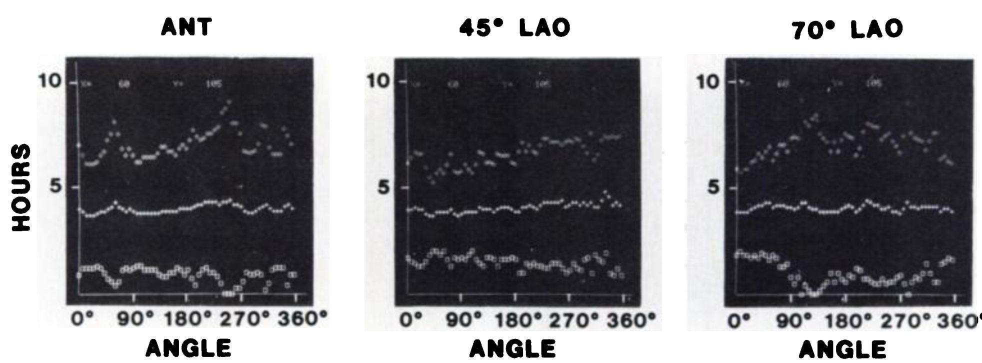

FIG. 4. Profiles representing mean effective half-times (shown with "+") and 2 s.d. above and below the mean for each 6° segment in each view. Note similarities between mean for each segment and mean for each view. Combined mean half-time was 3.97 ± 1.3 hr.

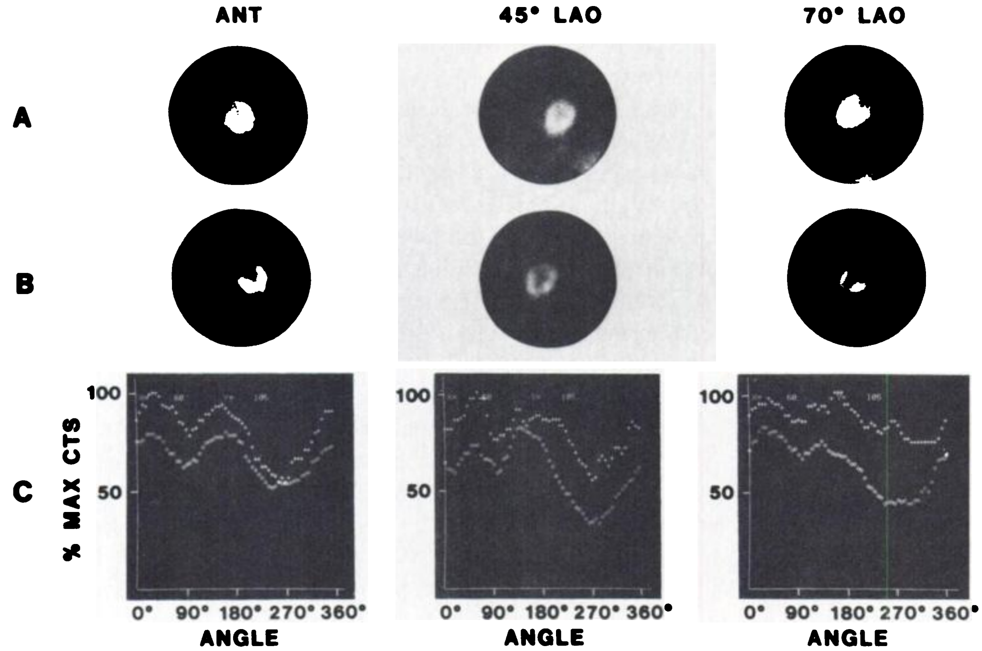

FIG. 5. Stress Tl-201 myocardial distribution in normal patient. Unprocessed stress images are shown in (A); corresponding computer-processed images in (B). Distribution circumferential profiles are plotted in (C) as upper curves, with lower limits of normal below. Note that no segment of distribution profile falls below lower limits of normal.

of modified interpolative background subtraction. As previously pointed out (9,11), quantitation of sequential images requires a method of systematically compensating for tissue crosstalk. Interpolative background subtraction provides the most satisfactory approach, since it accounts for nonuniformity in a background distribution that changes spatially and as a function of time in the delayed images. Therefore, methods that do not correct for tissue crosstalk (3,4), or those that use the subtraction of a constant (12), are not considered adequate.

To generate circumferential profiles, maximum counts per pixel along each radius were used, referenced from the visually located center of the left-ventricular cavity and aligned such that 90° in each view corresponded to the scintigraphic apex. The choice of maximal counts

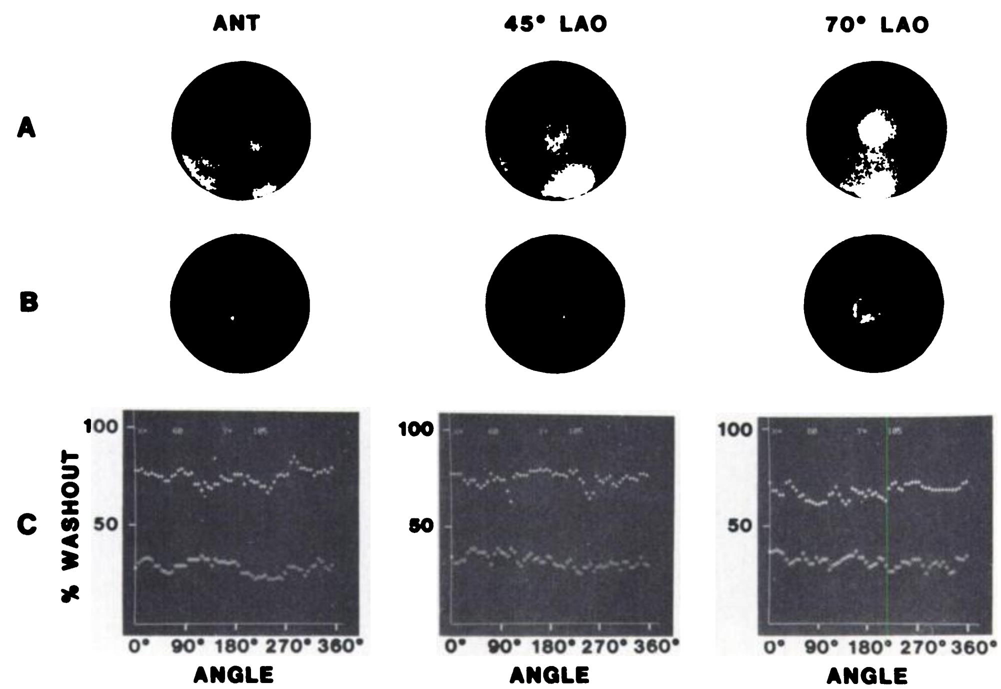

FIG. 6. Four-hour Tl-201 myocardial washout in normal patient of Fig. 5. Unprocessed delay images are shown in (A), and computer-processed in (B). Washout profiles (upper curves) plotted in (C) exhibit marked washout by 4 hr when compared with lower limits of normal (lower curves).

over average counts along a radius was based on the work of Vogel et al. (*13*), who determined that maximal circumferential profiles provided the most accurate measure of abnormality. Furthermore, the use of average counts in circumferential profile analysis has been found less sensitive than visual interpretation (*4*). The use of apex alignment was found to be of value by Burow et al. (*4*) for partial correction for variation in heart position. This alignment is particularly important, since the lower limits of the normal profiles vary for different angular locations in each view. For example, if in a normal study, the apex were misaligned, this region, which characteristically has the fewest counts, might fall below the lower limit of normal, causing a false abnormality. Methods that use lower limits of normal without proper alignment (*13*) are therefore limited.

Washout circumferential profiles were used to assess quantitatively the redistribution phenomenon. The technique is similar to that of Watson et al. (*9*) in that it quantitates relative washout that occurs between the stress and the delayed images. The mean effective half-time of Tl-201 in the myocardium observed by our technique (3.97 ± 1.3 hr) is in excellent agreement with the values reported by Watson et al. (*14*), who found a mean washout half-time of 3.98 ± 1.3 hr for the inferior wall, 3.85 ± 1.3 hr for the anterolateral wall, 4.17 ± 1.3 hr for anteroseptal wall, and 4.07 ± 1.6 hr for the posterolateral wall. The main differences between Watson's method and ours are that we image at 4 hr instead of 2 after injection, thus allowing a greater degree of washout to occur, and that our algorithm automatically calculates washout for each 6° location in each view, instead of relying on manually assigned profiles in preselected locations.

As predicted by Watson (*9*), the incorporation of washout abnormalities resulted in detection of additional patients with CAD as well as of additional abnormal segments not detected by the defect criteria alone. Of importance, none of these washout abnormalities could be detected by visual inspection of the scintigrams. This aspect of our quantitative analysis may prove to be the most important feature in increasing our ability to assess patients with balanced reduction of flow, such as may occur in three-vessel disease.

With respect to our extrapolation of normal limits established from images obtained 3–6 hr after injection to study washout at other times, we did encounter difficulty at less than 2.5 hr or more than 6 hr. Patients with imaging delay of less than 2.5 hr tended to demonstrate normal washout, since the extrapolated normal limits of washout were close to zero. Patients with imaging delay of greater than 6 hr tended to show abnormal washout, since after 6 hr the normal monoexponential washout assumption did not hold, and the normal washout rate became slower. We are currently applying an approach using multiexponential normal washout to our technique. Preliminary results suggest that between 3 and 7 hr the mean $t_{1/2}$ is 12.2 hr (*15*).

Some groups have described methods that use comparison of patient profiles with normal limits determined

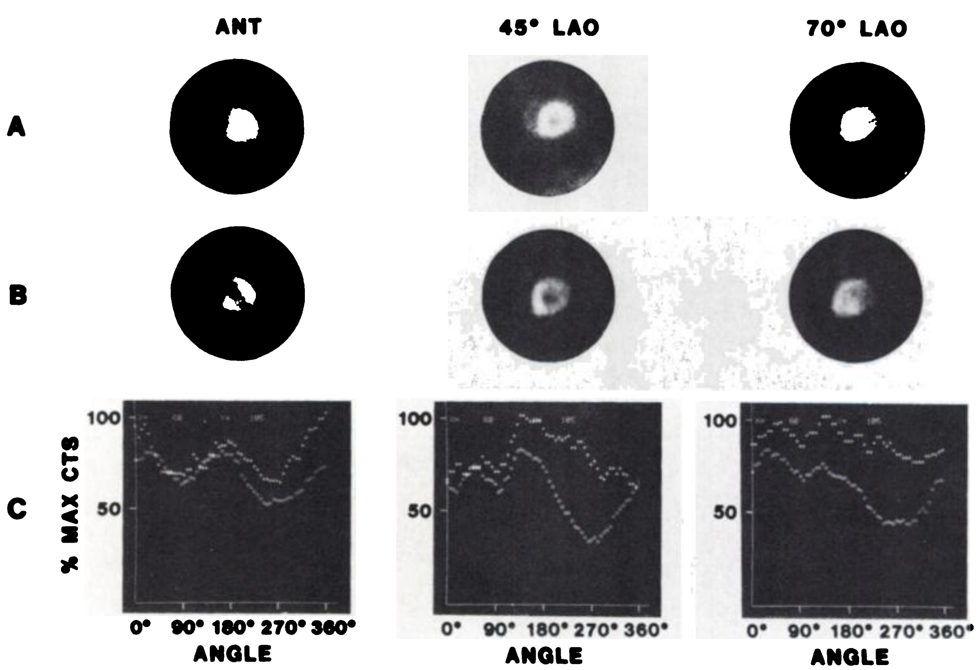

FIG. 7. Stress Tl-201 myocardial distribution of patient with triple-vessel CAD, who was diagnosed as normal by visual assessment of unprocessed images Figs. 7A and 8A. Differences in myocardial distribution between unprocessed (A) and processed (B) images are present. In the 45° LAO, processed images suggest a reversible defect in posterolateral wall. In anterior view the distribution profile, (C), ("+") falls below normal limits between 42 and 48° and between 126 and 132°. Neither segment is large enough to be interpreted by computer as an initial "defect."

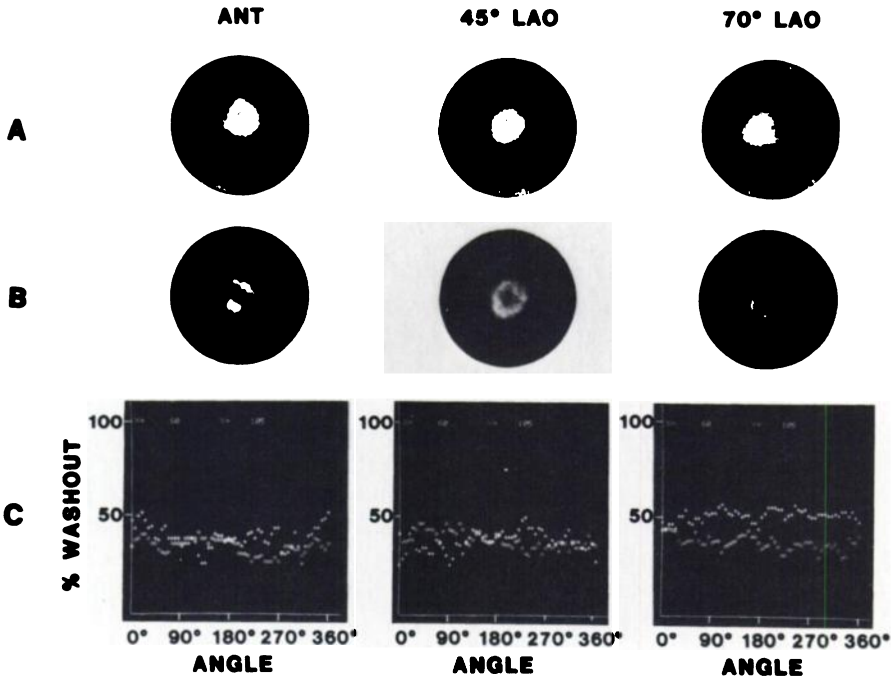

FIG. 8. Four-hour Tl-201 myocardial washout in the patient with triple-vessel disease from Fig. 7. Unprocessed (A) and processed (B) images, interpreted as normal, are shown. Part C exhibits washout abnormalities in distribution of all three major coronary arteries in anterior and 45° LAO views, indicated by segments of washout profiles ("+") falling below lower limits of normal.

from normal volunteers, or from patients having normal coronary arteriograms (*3,4,14*). An important difference in our approach is the selection of the normals from patients having less than 1% likelihood of coronary artery disease based on sequential Bayesian analysis. This approach avoids the pitfalls of using patients with normal coronary arteriograms who may have nonatherosclerotic ischemic disease (*5,16*). Furthermore, it allows the use of age-matched controls, which if attempted with "normal volunteers" might result in inclusion of an unacceptable proportion of patients with occult coronary disease.

Another reported approach has been the use of a defect-detecting threshold of 25% relative to the area of most intense uptake on the stress images. This threshold is used to determine significantly reduced segmental uptake (*5*). Our results in normal patients show that the lower limit of normal changes according to the view and the angular location in the myocardium. We found this lower limit to be as low as 45% below the maximum at the apex in the 45° LAO view, and as high as 20% below the maximum at the inferior wall in the anterior view.

The method presented showed excellent interobserver agreement, thus indicating a high degree of reproducibility. This important attribute is expected of an objective computerized method, particularly since the distribution and washout abnormalities are automatically detected by the computer. The method also proved to be accurate in separating normal patients from those with CAD. We should emphasize that the criteria described best separated normals from patients with CAD in our initial study group. A larger prospective evaluation is currently under way, in which we apply these criteria to assess sensitivity and specificity for detection of CAD and for the detection of individual coronary lesions (*17*).

TABLE 1.

View	Anterior			45° LAO			70° LAO			
Segment	Anterior	Apex	Inferior	Postero-lateral	Infero-apical	Septum	Inferior	Apex	Anterior	Total
Angle (degree)	330–54°	60–120°	126–210°	330–56°	60–120°	126–210°	330–54°	60–120°	126–210°	
Concordantly normal	7	8	8	8	8	8	9	9	8	73
Concordantly abnormal	2	3	3	2	3	2	1	1	3	20
Disagreement	2	0	0	1	0	1	1	1	0	6

Topics associated with this investigation that are in need of further study include: (a) the role that blood clearance of thallium plays in determining the rate of myocardial washout; (b) the effect of wall movement on counts per pixel in the myocardium, and whether gated thallium scintigraphy results in improved disease detection; (c) whether range rather than standard deviation should be used in defining the lower limits of normal (*15*); and (d) automated methods of assigning the center of the ventricle and the alignment of the curves. Furthermore, the technique can easily be modified to analyze the characteristics of Tl-201 lung distribution and washout, which may provide information regarding the severity of coronary disease (*18*).

This new, comprehensive computerized method offers promise to provide accurate, objective, reproducible assessment of the quantitative distribution and washout characteristics of thallium-201 in the myocardium.

ACKNOWLEDGMENTS

The authors gratefully acknowledge the research assistance of Nancy Pantaleo, David Brown and Ken Van Train, and the technical assistance of Evan Bullock-Morales and Fariba Assil.

This work was supported in part by Specialized Center of Research (SCOR) Grant No. HL 17651 from the National Heart, Lung, and Blood Institutes, NIH, Bethesda, Maryland, and by grants from the American Heart Association, Greater Los Angeles Affiliate.

This work was presented at the 27th Annual Meeting of the Society of Nuclear Medicine in Detroit, MI.

REFERENCES

1. Ritchie JL, Zaret BL, Strauss HW, et al: Myocardial imaging with thallium-201: a multicenter study in patients with angina pectoris or acute myocardial infarction. *Am J Cardiol* 42:345-350, 1978

2. Meade RC, Bamrah VS, Horgan JD, et al: Quantitative methods in the evaluation of thallium-201 myocardial perfusion images. *J Nucl Med* 19:1175-1178, 1978

3. Vogel RA, Kirch DL, LeFree MT, et al: Thallium-201 myocardial perfusion scintigraphy: results of standard and multi-pinhole tomographic techniques. *Am J Cardiol* 43: 787-793, 1979

4. Burow RD, Pond M, Schafer AW, et al: "Circumferential profiles:" a new method for computer analysis of thallium-201 myocardial perfusion images. *J Nucl Med* 20: 771-777, 1979

5. Berger BC, Watson DD, Burwell LR, et al: Redistribution of thallium at rest in patients with stable and unstable angina and the effect of coronary artery bypass surgery. *Circulation* 60:1114—1125, 1979

6. Diamond GA, Forrester JS: Analysis of probability as an aid in the clinical diagnosis of coronary-artery disease. *N Engl J Med* 300:1350-1358, 1979

7. Diamond GA, Chag M, Vas R, et al: Cardiokymography: quantitative analysis of regional ischemic left ventricular dysfunction. *Am J Cardiol* 41:1249-1257, 1978

8. Goris ML, Daspit SG, McLaughlin P, et al: Interpolative background subtraction. *J Nucl Med* 17:744-747, 1976

9. Watson DD, Beller GA, Berger BC, et al: Notes on the quantitation of sequential Tl-201 images. *Softwhere* 6:4-5, 10, 1979

10. Okada RD, Jacob ML, Newell JB, et al: Thallium-201 kinetics .in nonischemic canine myocardium. *Circulation* 60:II-172, 1979 (abst)

11. Goris ML: Nontarget activities: can we correct for them? *J Nucl Med* 20:1312-1314, 1979

12. Uhl GS, Kay TD: Computer analysis of thallium-201 myocardial perfusion scintigraphy: circumferential mapping. *Am J Cardiol* 45:481, 1980 (abst)

13. Vogel RA, Kirch DL, LeFree MT, et al: Improved diagnostic results of myocardial perfusion tomography using a new rapid inexpensive technique. *J Nucl Med* 19:730-731, 1978 (abst)

14. Watson DD, Campbell NP, Berger BC, et al: Quantitation of thallium-201 myocardial distribution and washout: normal standards for graded exercise studies. *Am J Cardiol* 45:480, 1980 (abst)

15. Garcia E, Maddahi J, Brown D, et al: Quantitative analysis of thallium-201 myocardial distribution and washout: Comparison of definition of normal. *Clin Res*, In Press

16. Fuller CM, Raizner AE, Chahine RA, et al: Exercise induced coronary artery spasm: angiographic demonstration, documentation of ischemia by myocardial scintigraphy and results of pharmacologic intervention.

17. Maddahi J, Garcia E, Berman D, et al: Quantitative analysis of stress and redistribution Tl-201 myocardial scintigrams improves detection and evaluation of extent of coronary artery disease. *J Nucl Med* 21:P51, 1980 (abst)

18. Boucher CA, Zir LM, Beller GA, et al: Increased lung uptake of thallium-201 during exercise myocardial imaging: clinical, hemodynamic and angiographic implications in patients with coronary artery disease. *Am J Cardiol* 46:189-196, 1980